COMPUTATIONAL PROBLEMS OF ELECTRICAL ENGINEERING
Vol. 2, No. 1, 2012

CURRENT DIFFERENTIAL RELAY WITH FAULT LOCATION AND SYNCHRONISATION OF MEASUREMENTS FUNCTIONS

Eugeniusz Rosolowski[1], Jan Izykowski[1], Murari Mohan Saha[2]
[1]Wroclaw University of Technology, Institute of Electrical Power Engineering, Wroclaw, Poland,
[2]ABB AB, Västerås, Sweden
eugeniusz.rosolowski@pwr.wroc.pl

Abstract: This paper considers a fault location and an analytical synchronisation of two-end measurements functions as embedded into a current differential protective relay. As a result of that, incomplete two-end measurements, i.e. a three-phase current measured at both line ends, while a three-phase voltage only from one end are considered as the input signals. The fault location and synchronisation formulae are derived with considering a distributed-parameter model of a transposed overhead line. The performed ATP-EMTP based evaluation has proved the validity of the presented algorithms and their high accuracy.

Key words: overhead power line, current differential relay, fault location, two-end measurement, analytic synchronisation, ATP-EMTP software.

1. Introduction

A number of concepts are utilised in protective relaying of power systems, yet a unit protection is considered as the most efficient one. Such the concept results in the individual protection of sections of a power system. A current differential relay [1]–[5] is the unit protection system which is used most frequently. Its principle is to sense the difference between the incoming and outgoing terminal currents of the protected section. This method is used for protecting power transformers, generators, generator-transformer units, motors, bus-bars and power lines.

The considerations of this paper are focused on increasing the functionality of a current differential relay designated for protecting long overhead transmission lines (Fig. 1). In particular, equipping a relay with the functions of:

- the fault location for an inspection-repair purpose [6],
- the synchronisation of two-end measurements [4].

Power transmission lines are distinctive from the other power system components by their longitudinal size. Because of long distances between line ends the extra media for information interexchange is required and sophisticated methods of two-end measurement data alignment are applied. One of the most effective solutions is a 'ping-pong' algorithm [1]. The transmitted data are stamped locally with time tags which allow for estimation of an actual delay in both directions even in case of channel propagation time asymmetry. The most precise method of delay compensation and sampling synchronization is based on the satellite Global Positioning System (GPS) [2]–[3]. However, reliance on the system independent of the protection system owner is not an optimal solution. Therefore, in this paper a fault location function is considered to be performed while utilising two-end unsynchronised measurements. This makes a substantial difference in comparison to the earlier approach presented in [5] where the considerations were carried out under the assumption that the measurements are perfectly synchronised.

This paper presents a new algorithm for locating faults on a two-terminal power transmission line. It is assumed here (Fig. 1) that a fault locator (FL) is embedded into a current differential relay in the terminal A. Besides the phasors of the three-phase current (of the phases: a, b, c – as denoted in the subscripts) from the end A: $\{\underline{I}_A\}=\{\underline{I}_{Aa}, \underline{I}_{Ab}, \underline{I}_{Ac}\}$ and those from the end B: $\{\underline{I}_B\}=\{\underline{I}_{Ba}, \underline{I}_{Bb}, \underline{I}_{Bc}\}$, which are utilised by the relay, the fault locator is additionally supplied with the three-phase voltage $\{v_A\}=\{v_{Aa}, v_{Ab}, v_{Ac}\}$ from the local line end (A). Thus, the fault locator is designed to utilise the communication infrastructure of the current differential relays, thus not demanding additional communication links. As a result, the current differential relay besides its main feature, i.e. indicating whether a fault occurred within a line or outside it, provides also the information on the accurate position of the fault, which is required for the inspection-repair purpose [6].

With the aim of providing high accuracy for locating faults on long lines, the distributed-parameter line model (Fig. 2) is strictly utilised in the presented algorithms. Both, the voltage drop across the faulted line segment and also across the fault path resistance are determined with strict consideration of the distributed parameter line model.

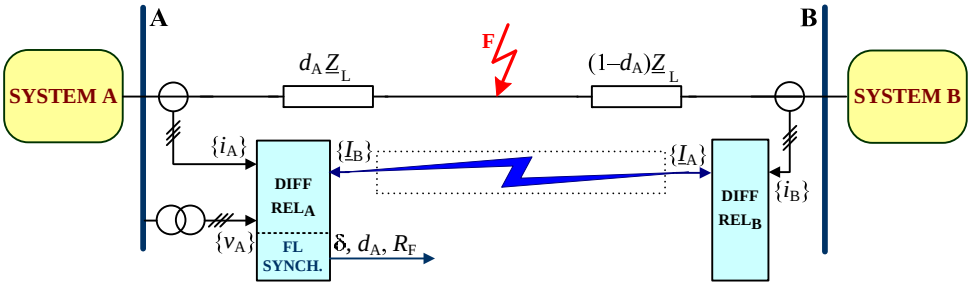

Fig. 1. Fault location (FL) and synchronisation (SYNCH.) associated with differential relays of power line

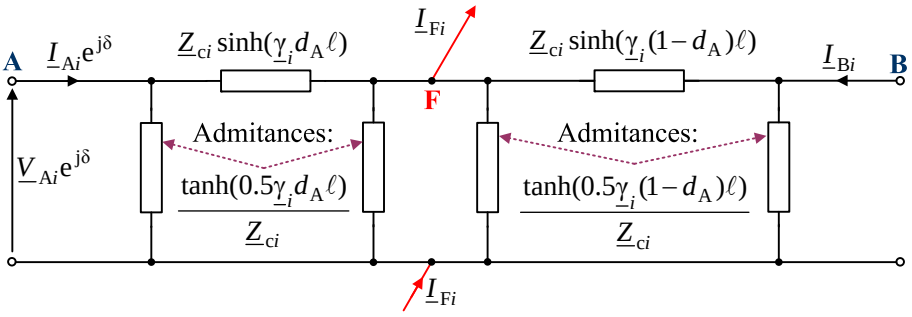

Fig. 2. Distributed-parameter model of a faulted line for the i-th symmetrical components sequence

In this paper, use of incomplete two-end unsynchronised measurements [6] is considered. Due to insufficient measurement data, instead of processing the signals of the individual symmetrical components, the natural fault loops are to be considered. Accordingly to the identified fault type, the single phase loop (for phase-to-ground faults) and inter-phase loop (for faults involving two or three phases) have to be considered. The fault loop contains the section of the line from the measuring point (A) up to the fault point (F) and the fault path resistance.

The paper starts with derivation of the fault location algorithm. Then, the results for the example fault, using the signals from ATP-EMTP simulation [7], are presented and discussed.

2. Fault location algorithm

2.1. Generalised fault loop model

The generalised fault loop model [6], which in the considered case describes the fault loop seen from the line end A is presented as follows:

$$\underline{V}_{Fp}(d_A) - R_F\underline{I}_F = 0 \qquad (1)$$

where: $\underline{V}_{Fp}(d_A)$ is a fault loop voltage between the fault locator installation point (the bus A) and the fault point F composed of its symmetrical components accordingly to the fault type; d_A is an unknown relative distance to the fault (p.u.), R_F is a fault path resistance; $\underline{I}_F$ is a total fault current (fault path current).

2.2. Fault loop voltage at fault point

The original fault loop voltage between the bus A and the fault point F can be represented using a weighted sum of the respective symmetrical components:

$$\underline{V}_{Fp}(d_A) = \underline{a}_1\underline{V}_{F1} + \underline{a}_2\underline{V}_{F2} + \underline{a}_0\underline{V}_{F0} \qquad (2)$$

where: subscripts denoting the component type are as follows: 1 – positive-, 2 – negative-, 0 – zero-sequence, $\underline{a}_1$, $\underline{a}_2$, $\underline{a}_0$ are weight coefficients dependent on a fault type [6], as shown in Table 1.

Table 1

Weight coefficients for composing a fault loop voltage (2)

Fault Type	$\underline{a}_1$	$\underline{a}_2$	$\underline{a}_0$
a–g	1	1	1
b–g	$\underline{a}^2$	$\underline{a}$	1
c–g	$\underline{a}$	$\underline{a}^2$	1
a–b, a–b–g a–b–c, a–b–c–g	$1-\underline{a}^2$	$1-\underline{a}$	0
b–c, b–c–g	$\underline{a}^2-\underline{a}$	$\underline{a}-\underline{a}^2$	0
c–a, c–a–g	$\underline{a}-1$	$\underline{a}^2-1$	0
$\underline{a}=\exp(j2\pi/3)$; $j=\sqrt{-1}$			

Applying the distributed-parameter line model [6], the symmetrical components of voltages from (2) are determined as follows:

$$\underline{V}_{F1} = [\underline{V}_{A1}\cosh(\underline{\gamma}_1 \ell d_A) - \underline{Z}_{c1}\underline{I}_{A1}\sinh(\underline{\gamma}_1 \ell d_A)]e^{j\delta} \quad (3)$$

$$\underline{V}_{F2} = [\underline{V}_{A2}\cosh(\underline{\gamma}_1 \ell d_A) - \underline{Z}_{c1}\underline{I}_{A2}\sinh(\underline{\gamma}_1 \ell d_A)]e^{j\delta} \quad (4)$$

$$\underline{V}_{F0} = [\underline{V}_{A0}\cosh(\underline{\gamma}_0 \ell d_A) - \underline{Z}_{c0}\underline{I}_{A0}\sinh(\underline{\gamma}_0 \ell d_A)]e^{j\delta} \quad (5)$$

where: $e^{j\delta}$ is a synchronisation operator (δ is an unknown synchronisation angle) ensuring the common time base of digital measurements from the buses A and B [6], $\underline{V}_{A1}$, $\underline{V}_{A2}$, $\underline{V}_{A0}$ are symmetrical components of the side A voltage, $\underline{I}_{A1}$, $\underline{I}_{A2}$, $\underline{I}_{A0}$ are symmetrical components of the side A current, ℓ is the length of the line (km), $\underline{\gamma}_1 = \sqrt{\underline{Z}'_{1L}\underline{Y}'_{1L}}$ is the propagation constant of the line for the positive- (negative-) sequence, $\underline{\gamma}_0 = \sqrt{\underline{Z}'_{0L}\underline{Y}'_{0L}}$ is the propagation constant of the line for the zero-sequence, $\underline{Z}_{c1} = \sqrt{\underline{Z}'_{1L}/\underline{Y}'_{1L}}$ is the characteristic impedance of the line for the positive-sequence (negative-sequence), $\underline{Z}_{c0} = \sqrt{\underline{Z}'_{0L}/\underline{Y}'_{0L}}$ is the characteristic impedance of the line for the zero-sequence, $\underline{Z}'_{1L} = R'_{1L} + j\omega_1 L'_{1L}$ is the impedance of the line for the positive-sequence (negative-sequence) (Ω/km), $\underline{Z}'_{0L} = R'_{0L} + j\omega_1 L'_{0L}$ is the impedance of the line for the zero-sequence (Ω/km), $\underline{Y}'_{1L} = G'_{1L} + j\omega_1 C'_{1L}$ is the admittance of the line for the positive-sequence (negative-sequence) (S/km), $\underline{Y}'_{0L} = G'_{0L} + j\omega_1 C'_{0L}$ is the admittance of the line for the zero-sequence (S/km), R'_{1L}, L'_{1L}, G'_{1L}, C'_{1L} are the resistance, inductance, conductance, and capacitance of the line for the positive-sequence (negative-sequence) per km length, R'_{0L}, L'_{0L}, G'_{0L}, C'_{0L} are the resistance, inductance, conductance, and capacitance of the line for the zero-sequence per km length.

The line parameters for the positive- and negative-sequences are identical and therefore they are uniformly denoted with '1' in the subscripts for both sequences.

2.3. Total fault current

Summing phase currents (from phases: a, b, c) from both line ends (A and B) appears to be the simplest way to determine the fault current in the particular phases at the fault point. However, this way does not take into consideration the currents charging line shunt capacitances. This is the explanation why this way to determine the total fault current is not used here. Instead, a detailed analysis of the flow of currents in the faulted line is considered.

Taking into account the share of individual symmetrical components (denoted with the subscripts: 1 – positive-, 2 – negative-, 0 – zero-sequence, respectively): $\underline{I}_{F1}$, $\underline{I}_{F2}$, $\underline{I}_{F0}$, one obtains [5]–[6]:

$$\underline{I}_F = \underline{a}_{F1}\underline{I}_{F1} + \underline{a}_{F2}\underline{I}_{F2} + \underline{a}_{F0}\underline{I}_{F0} \quad (6)$$

where: $\underline{a}_{F1}$, $\underline{a}_{F2}$, $\underline{a}_{F0}$ are share coefficients, dependent on a fault type and the assumed preference with respect to using particular sequences (the recommended set is delivered in Table 2).

Table 2

Share coefficients for composing a total fault current (6)

Fault Type	$\underline{a}_{F1}$	$\underline{a}_{F2}$	$\underline{a}_{F0}$
a–g	0	3	0
b–g	0	$3\underline{a}$	0
c–g	0	$3\underline{a}^2$	0
a–b	0	$1-\underline{a}$	0
b–c	0	$\underline{a}-\underline{a}^2$	0
c–a	0	$\underline{a}^2-1$	0
a–b–g	$1-\underline{a}^2$	$1-\underline{a}$	0
b–c–g	$\underline{a}^2-\underline{a}$	$\underline{a}-\underline{a}^2$	0
c–a–g	$\underline{a}-1$	$\underline{a}^2-1$	0
a–b–c, a–b–c–g	$1-\underline{a}^2$	$1-\underline{a}$ *)	0

*) – there is no negative sequence component under these faults and the coefficient can be assumed equal to zero

There is a possibility of applying different, alternative sets of the share coefficients [5]–[6], however, the coefficients for which the zero-sequence is eliminated ($\underline{a}_{F0} = 0$) – as in Table 2, have been recommended for the considered fault location algorithm. In this way, using of zero-sequence line parameters (which are considered to be unreliable data) is avoided while determining the total fault current. This is advantageous for assuring the highest possible accuracy of the fault location.

It is important that for the share coefficients proposed in Table 2 the preference of using the negative-sequence over the positive-sequence has been set for single-phase and phase-to-phase faults.

The accurate determination of symmetrical components of a total fault current can be performed with the strict consideration of the distributed-parameter model of a faulted line (Fig. 2). Taking this model into the consideration, one derives the following formula for the *i*-th symmetrical component of the total fault current [6]:

$$\underline{I}_{\mathrm{F}i} = \frac{\underline{M}_i(\mathrm{e}^{\mathrm{j}\delta})}{\underline{Z}_{ci}\cosh(\underline{\gamma}_i \ell(1-d_{\mathrm{A}}))} \tag{7}$$

where:

$$\underline{M}_i(\mathrm{e}^{\mathrm{j}\delta}) = \underline{Z}_{ci}\underline{I}_{\mathrm{B}i} + \underline{N}_{\mathrm{A}i}\mathrm{e}^{\mathrm{j}\delta}$$

$$\underline{N}_{\mathrm{A}i} = \underline{Z}_{ci}\underline{I}_{\mathrm{A}i}\cosh(\underline{\gamma}_i \ell) - \underline{V}_{\mathrm{A}i}\sinh(\underline{\gamma}_i \ell)$$

i=1: positive-sequence, i=2: negative-sequence and: i=0: zero-sequence.

The obtained formula (7) for the i-th symmetrical component of the total fault current is compact and the unknown distance to fault (d_{A}) is involved in the denominator, while the synchronisation operator (exp(j)) in the nominator of (7) only.

Substituting the positive- and negative-sequence components of the total fault current, determined in [7], into (6), and also taking into account that the zero-sequence has been eliminated (Table 2), one obtains the total fault current in the form:

$$\underline{I}_{\mathrm{F}} = \frac{\underline{a}_{\mathrm{F1}}\underline{M}_1(\mathrm{e}^{\mathrm{j}\delta}) + \underline{a}_{\mathrm{F2}}\underline{M}_2(\mathrm{e}^{\mathrm{j}\delta})}{\underline{Z}_{\mathrm{c1}}\cosh(\underline{\gamma}_1 \ell(1-d_{\mathrm{A}}))} \tag{8}$$

The substitution of the total fault current (8) into the generalised fault loop model (1) yields:

$$\underline{V}_{\mathrm{Fp}}(d_{\mathrm{A}}) - R_{\mathrm{F}}\frac{\underline{a}_{\mathrm{F1}}\underline{M}_1(\mathrm{e}^{\mathrm{j}\delta}) + \underline{a}_{\mathrm{F2}}\underline{M}_2(\mathrm{e}^{\mathrm{j}\delta})}{\underline{Z}_{\mathrm{c1}}\cosh(\underline{\gamma}_1 \ell(1-d_{\mathrm{A}}))} = 0 \tag{9}$$

where $\underline{V}_{\mathrm{Fp}}(d_{\mathrm{A}})$ has been defined in (2)–(5), with use of the weight coefficients specified for different faults in Table 1, $\underline{M}_1(\mathrm{e}^{\mathrm{j}\delta})$, $\underline{M}_2(\mathrm{e}^{\mathrm{j}\delta})$ have been defined in (7), $\underline{a}_{\mathrm{F1}}$, $\underline{a}_{\mathrm{F2}}$ are share coefficients dependent on the fault type, as shown in Table 2.

The derived fault location formula (9) is compact and covers different fault types, what requires setting the appropriate fault type coefficients provided in Table 1 and Table 2.

There are three unknown variables in the fault location formula (9): the distance to a fault (d_{A}), a fault resistance (R_{F}) and a synchronisation angle ( ). In order to solve the equation with such number of unknowns, an additional equation involving the synchronisation angle has to be formulated. For this purpose the boundary conditions of different fault types are considered.

After excluding the zero sequence components ($\underline{a}_{\mathrm{F0}}$=0 in Table 2) the total fault current is equal:

$$\underline{I}_{\mathrm{F}} = \underline{a}_{\mathrm{F1}}\underline{I}_{\mathrm{F1}} + \underline{a}_{\mathrm{F2}}\underline{I}_{\mathrm{F2}} \tag{10}$$

There are two characteristic sets (among the other possible) of the share coefficients for the phase-to-ground and phase-to-phase faults, shown in Table 3.

Table 3

Two sets of share coefficients for phase-to-ground faults and phase-to-phase faults

Fault Type	I–SET		II–SET	
	$\underline{a}_{\mathrm{F1}}^{\mathrm{I–SET}}$	$\underline{a}_{\mathrm{F2}}^{\mathrm{I–SET}}$	$\underline{a}_{\mathrm{F1}}^{\mathrm{II–SET}}$	$\underline{a}_{\mathrm{F2}}^{\mathrm{II–SET}}$
a–g	0	3	3	0
b–g	0	$3\underline{a}$	$3\underline{a}^2$	0
c–g	0	$3\underline{a}^2$	$3\underline{a}$	0
a–b	0	$1-\underline{a}$	$1-\underline{a}^2$	0
b–c	0	$\underline{a}-\underline{a}^2$	$\underline{a}^2-\underline{a}$	0
c–a	0	$\underline{a}^2-1$	$\underline{a}-1$	0

Applying the sets from Table 3 one can express the total fault current as follows:

$$\underline{I}_{\mathrm{F}} = \underline{a}_{\mathrm{F1}}^{\mathrm{I–SET}}\underline{I}_{\mathrm{F1}} + \underline{a}_{\mathrm{F2}}^{\mathrm{I–SET}}\underline{I}_{\mathrm{F2}} \tag{11}$$

or alternatively:

$$\underline{I}_{\mathrm{F}} = \underline{a}_{\mathrm{F1}}^{\mathrm{II–SET}}\underline{I}_{\mathrm{F1}} + \underline{a}_{\mathrm{F2}}^{\mathrm{II–SET}}\underline{I}_{\mathrm{F2}} \tag{12}$$

Comparing (11) with (12) and taking into account (7) one gets the following formula for the synchronisation operator for the faults in Table 3:

$$[\mathrm{e}^{\mathrm{j}\delta}]_{\mathrm{ph-g,\,ph-ph}} = \frac{\underline{Z}_{\mathrm{c1}}(\underline{a}_{\mathrm{F2}}^{\mathrm{I–SET}}\underline{I}_{\mathrm{B2}} - \underline{a}_{\mathrm{F1}}^{\mathrm{II–SET}}\underline{I}_{\mathrm{B1}})}{\underline{a}_{\mathrm{F1}}^{\mathrm{II–SET}}\underline{N}_{\mathrm{A1}} - \underline{a}_{\mathrm{F2}}^{\mathrm{I–SET}}\underline{N}_{\mathrm{A2}}} \tag{13}$$

In case of phase-to-phase-to-ground faults the analysis of the boundary conditions yields the following relation between the symmetrical components of the total fault current [6]:

$$\underline{I}_{\mathrm{F0}} = \underline{b}_{\mathrm{F1}}\underline{I}_{\mathrm{F1}} + \underline{b}_{\mathrm{F2}}\underline{I}_{\mathrm{F2}} \tag{14}$$

where $\underline{b}_{\mathrm{F1}}$, $\underline{b}_{\mathrm{F2}}$ are the coefficients delivered in Table 4.

Table 4

Coefficients involved in the expression (14)

Fault Type	$\underline{b}_{\mathrm{F1}}$	$\underline{b}_{\mathrm{F2}}$
a–b–g	$-\underline{a}$	$-\underline{a}^2$
b–c–g	–1	–1
c–a–g	$-\underline{a}^2$	$-\underline{a}$

Substituting (7) into (14) results in:

$$\frac{\underline{Z}_{\mathrm{c0}}\underline{I}_{\mathrm{B0}} + \underline{N}_{\mathrm{A0}}[\mathrm{e}^{\mathrm{j}\delta}]_{\mathrm{ph-ph-g}}}{\underline{Z}_{\mathrm{c0}}\cosh(\underline{\gamma}_0 \ell(1-d_{\mathrm{A}}))} = \frac{\underline{Z}_{\mathrm{c1}}(\underline{b}_{\mathrm{F1}}\underline{I}_{\mathrm{B1}} + \underline{b}_{\mathrm{F2}}\underline{I}_{\mathrm{B2}}) + (\underline{b}_{\mathrm{F1}}\underline{N}_{\mathrm{A1}} + \underline{b}_{\mathrm{F2}}\underline{N}_{\mathrm{A2}})[\mathrm{e}^{\mathrm{j}\delta}]_{\mathrm{ph-ph-g}}}{\underline{Z}_{\mathrm{c1}}\cosh(\underline{\gamma}_1 \ell(1-d_{\mathrm{A}}))} \tag{15}$$

For three-phase balanced faults one can derive for the pre-fault state (superscript: pre) positive-sequence:

$$[\mathrm{e}^{\mathrm{j}\delta}]_{\mathrm{3ph}} = \frac{-\underline{Z}_{\mathrm{c1}}\underline{I}_{\mathrm{B1}}^{\mathrm{pre}}}{\sinh(\underline{\gamma}_1 \ell)\underline{V}_{\mathrm{A1}}^{\mathrm{pre}} + \underline{Z}_{\mathrm{c1}}\cosh(\underline{\gamma}_1 \ell)\underline{I}_{\mathrm{A1}}^{\mathrm{pre}}} \tag{16}$$

The distance to the fault is not involved in the determination of the synchronisation operator (16).

After decomposing (9) into its real and imaginary parts and taking one of the relations: either (13), or (15), or (16), respectively, we can apply one of the known numeric procedures for solving nonlinear equations. It has been verified that the Newton-Raphson iterative method is a good choice for that.

3. ATP-EMTP based evaluation

The performance of the presented method has been analysed using a digital model running on ATP-EMTP simulation software program [7]. A single-circuit transmission line has been used in the simulation. The main parameters of the modelled transmission system are as follows:

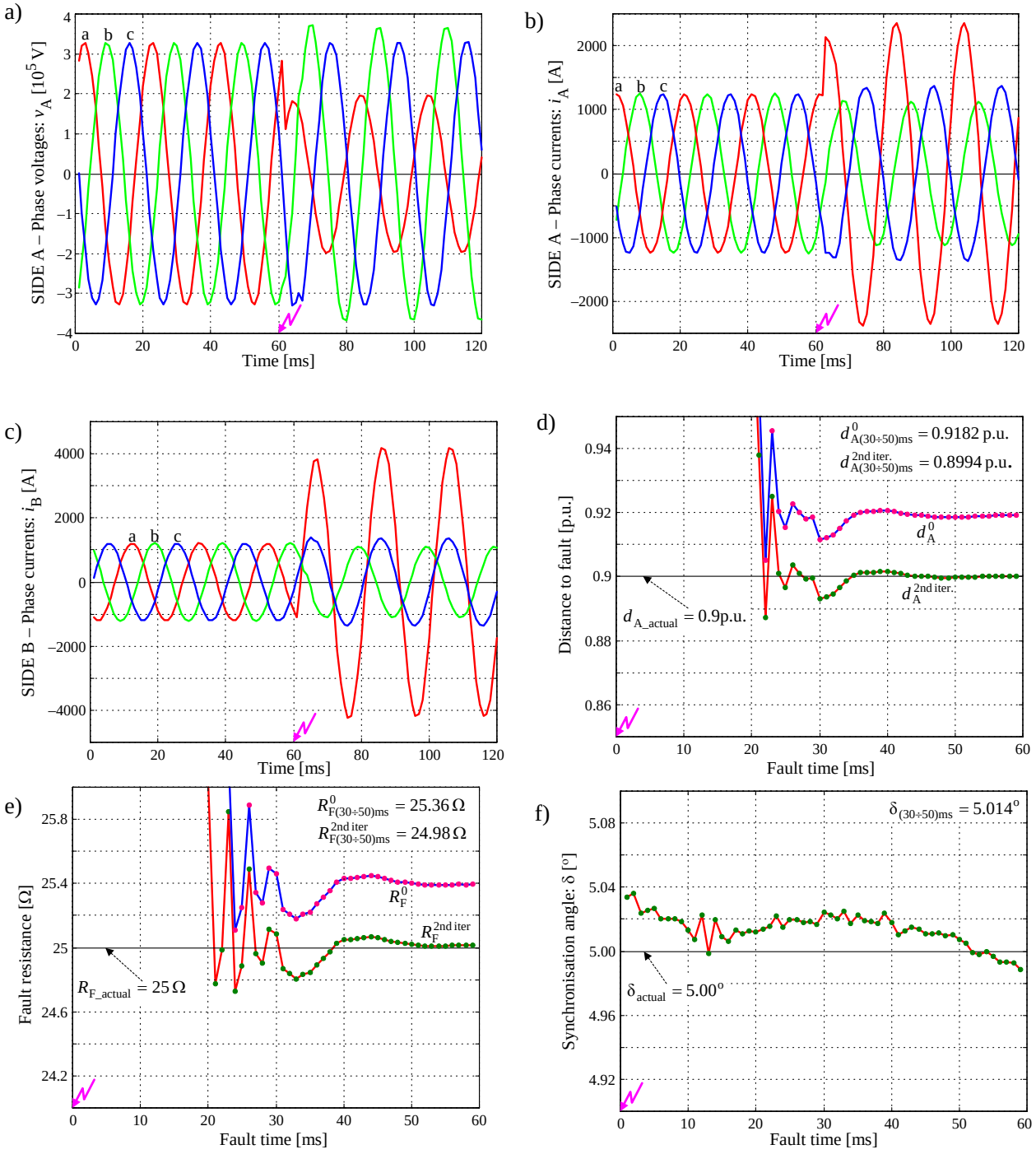

Fig. 3. The sample fault example: a) three-phase voltage of side A, b) three-phase current of side A, c) three-phase current of side B, d) calculated distance to fault, e) calculated fault resistance, f) calculated synchronization angle

- rated voltage: 400kV
- line length: 300km
- system frequency: 50 Hz
- phase angle of EMFs of systems: A: 0^o, B: (-30^o)
- sequence impedances of equivalent systems:
  $\underline{Z}_{1SA}=\underline{Z}_{1SB}=(1.307+j15)$ $\underline{Z}_{0SA}=\underline{Z}_{0SB}=(2.318+j26.5)$
- line impedances:
  $\underline{Z}_{1L}=(0.0267+j0.3151)\Omega/km$
  $\underline{Z}_{0L}=(0.275+j1.026)\Omega/km$
- line shunt capacitances:
  $C_{1L}=0.013\mu F/km$, $C_{0L}=0.0085\mu F/km$.

Different scenarios of faults have been considered in the performed evaluation study. A fault type, a fault resistance and equivalent system impedances have been changed. Deliberately a de-synchronisation of measurements has been introduced. The obtained results for the distance to a fault, the fault resistance and the synchronisation angle of all test cases are correct and accurate.

Fig. 3 presents measured three-phase signals and calculation results for a sample single phase a–g fault. The following specifications for this fault have been taken: d_{A_actual} =0.9p.u., R_{F_actual} =25Ω, $\delta_{actual}=5^o$. The measurements from the bus A have been deliberately delayed by 5^o with respect to the measurement of the current from the remote line end (B).

In Fig. 3a–3c the three-phase measured signals are shown. For the applied comparatively high fault resistance (25Ω) there are no visible d.c. components in phase currents. The distance to the fault (Fig. 3d) and the fault resistance (Fig. 3e) have been obtained in the course of iterative calculations. The start of these calculations (iteration number '0') was given by transferring the equations to the form relevant for a lumped-parameter line model. Such simplification has caused some errors in calculated results. For example, the distance to the fault averaged within the interval from 30 to 50 ms of the fault time: $d^{0}_{A(30\div50)ms}=0.9182$ p.u. differs by around 2% from the actual result (0.9 p.u.). However, after performing two iterations (superscript: '2nd iter') a very accurate result: $d^{2nd\ iter}_{A(30\div50)ms}=0.8994$ p.u. has been obtained. The synchronisation angle determined for this fault type according to (13): $\delta=5.014^o$ is very close to the introduced de-synchronisation (5.000^o).

Different specifications of faults and pre-fault power flows have been considered in the evaluation of the accuracy of the developed fault location algorithm. For the faults involving a fault resistance up to 25 Ω, maximum errors do not exceed: 0.25% for the case of the instrument transformers with ideal transformation and 1.5% for the case with real instrument transformers included.

4. Conclusions

A new fault location algorithm utilising unsynchronised measurements of two-end currents and one-end voltage is presented. It has been assumed that such fault location algorithm has been incorporated into a current differential relay. In this way, the communication between the line ends of differential relays has been utilised. By embedding the fault location and the analytic synchronisation of measurements functions into the relay, an increase of the relay functionality has been simply achieved.

Compact forms of the equations for the fault location and the synchronisation angle determination have been obtained. They are valid for different fault types and this is reflected by setting appropriate fault type coefficients. The high accuracy of the fault location is assured by strict considering of the distributed-parameter line model. The solution of the derived equations has been obtained with the Newton-Raphson iterative calculations.

The performed evaluation with use of the fault data obtained from versatile simulation of faults on the test transmission network with a single-circuit long transmission line has proved that the derived algorithms can be effectively applied to increase the functionality of protective differential relays. The included fault example illustrates very good performance of the developed algorithms.

Acknowledgments

The authors are grateful for the support of the Ministry of Science and Higher Education of Poland under Grant N N511 303638 conducted in years 2010–2012.

References

1. Mills D. L. Internet Time Synchronization: The Network Time Protocol // IEEE Transactions on Communications. – 1991. – Vol. 39, No. 10.

2. Hall I., Beaumont P. G., Baber G. P., Shuto I., Saga M., Okuno K., Ito H. New line current differential relay using GPS synchronization // Proceedings of IEEE Bologna PowerTech Conference. – 2003.

3. Li H. Y., Southern E. P., Crossley P. A., Potts S., Pickering S. D. A., Caunce B. R. J., Weller G. C. A new type of differential feeder protection relay using the Global Positioning System for data synchronization // IEEE Trans. on Power Delivery. – 1997. – Vol. 12, No 3. –P. 1090–1099.

4. Lukowicz M. New method of data transmission delay estimation for feeder differential protection, Present Problems of Power System Control. – Wroclaw: Oficyna Wydawnicza Politechniki Wroclawskiej, , Poland. – 2011. – P. 97–107.

5. Rosolowski E., Izykowski J., and Saha M. M.: Using of current differential protection signals for fault

location on two-terminal line // Przeglad Elektrotechniczny.– 2008.– No 5. – P. 9–13.

6. Saha M. M., Izykowski J., Rosolowski E. Fault location on power networks. – Springer-Verlag, London, Series: Power Systems. – 2010.

7. Dommel H. Electro-Magnetic Transients Program. – Bonneville Power Administration, Portland, OR. – 1986.

СТРУМОВЕ ДИФЕРЕНЦІЙНЕ РЕЛЕ ІЗ ВБУДОВАНОЮ ПРОЦЕДУРОЮ ЛОКАЛІЗАЦІЇ НЕСПРАВНОСТІ ТА СИНХРОНІЗАЦІЇ ВИМІРЯНИХ ФУНКЦІЙ

Е. Росоловскі, Я. Ізиковскі,
M. M. Cara

У статті розглядається процедура локалізації несправності та аналітичної синхронізації виміряних на двох кінцях функцій, вбудована у струмове диференційне реле захисту. В результаті цього використовуються неповні вимірювання, проведені на двох кінцях лінії, наприклад, трифазний струм, виміряний на обох кінцях лінії, та трифазна напруга, виміряна лише на одному кінці, подаються як вхідні сигнали. Алгоритм локалізації та формулу синхронізації отримано на підставі моделювання транспонованої повітряної лінії схемою з розподіленими параметрами. Розрахунки, проведені з допомогою ATP-EMTP, підтвердили адекватність запропонованих алгоритмів та їх точність.

Eugeniusz Rosolowski – M'1997, SM'2000 – was born in Poland in 1947. He received his M.Sc. degree in Electrical Eng. from the Wroclaw University of Technology (WUT) in 1972. From 1974 to 1977, he studied in Kiev Politechnical Institute, where he received Ph.D. in 1978. In 1993 he received D.Sc. from the WUT. Presently he is a Professor in the Institute of Electrical Engineering. His research interests are in power system analysis and microprocessor applications in power systems. He is a holder of about 25 patents and authored more than 250 technical papers. He is the co-author of a book entitled "Fault Location on Power Networks", published by Springer, January 2010.

Jan Izykowski – M'1997, SM'04 was born in Poland in 1949. He received his M.Sc., Ph.D. and D.Sc. degrees from the Faculty of Electrical Engineering of Wroclaw University of Technology (WUT) in 1973, 1976 and in 2001, respectively. In 1973 he joined Institute of Electrical Power Engineering of the WUT where he is presently a.Professor and Director of this Institute. His research interests are in the simulation of power system transients, in power system protection and control, and fault location. He is a holder of 20 patents and has authored more than 200 technical papers. He is the co-author of a book entitled "Fault Location on Power Networks", published by Springer, January 2010

Murari Mohan Saha – M´1976, SM´1987 – was born in 1947 in Bangladesh. He received B.Sc.E.E. from Bangladesh University of Engineering and Technology (BUET), Dhaka in 1968 and completed M.Sc.E.E. in 1970.

From 1969 to 1971 he was a lecturer at the department of Electrical Engineering at BUET, Dhaka. In 1972, he completed M.S.E.E. and in 1975 he was awarded with Ph.D. from the Technical University of Warsaw, Poland. He joined ASEA, Sweden, in 1975 as a Development Engineer and currently is a Senior Research and Development Engineer at ABB AB, Västerås, Sweden. He is a Senior Member of IEEE and a Fellow of IET (UK). He is a registered European Engineer (EUR ING) and a Chartered Engineer (C Eng). His areas of interest are measuring transformers, power system analysis and simulation, digital protective relays. He holds about 35 patents and has authored more than 200 technical papers. He is the co-author of a book entitled "Fault Location on Power Networks", published by Springer, January 2010.